TU Delft

Delft University of Technology

Scaling of flow curves

Comparison between experiments and simulations

Dekker, Riande I.; Dinkgreve, Maureen; Cagny, Henri de; Koeze, Dion J.; Tighe, Brian P.; Bonn, Daniel

DOI
10.1016/j.jnnfm.2018.08.006

Publication date
2018

Document Version
Final published version

Published in
Journal of Non-Newtonian Fluid Mechanics

Citation (APA)
Dekker, R. I., Dinkgreve, M., Cagny, H. D., Koeze, D. J., Tighe, B. P., & Bonn, D. (2018). Scaling of flow curves: Comparison between experiments and simulations. *Journal of Non-Newtonian Fluid Mechanics*, *261*, 33-37. https://doi.org/10.1016/j.jnnfm.2018.08.006

Important note
To cite this publication, please use the final published version (if applicable).
Please check the document version above.

Copyright
Other than for strictly personal use, it is not permitted to download, forward or distribute the text or part of it, without the consent of the author(s) and/or copyright holder(s), unless the work is under an open content license such as Creative Commons.

Takedown policy
Please contact us and provide details if you believe this document breaches copyrights.
We will remove access to the work immediately and investigate your claim.

This work is downloaded from Delft University of Technology.
For technical reasons the number of authors shown on this cover page is limited to a maximum of 10.

Journal of Non-Newtonian Fluid Mechanics 261 (2018) 33–37

Contents lists available at ScienceDirect

Journal of Non-Newtonian Fluid Mechanics

journal homepage: www.elsevier.com/locate/jnnfm

Scaling of flow curves: Comparison between experiments and simulations

Riande I. Dekker[a], Maureen Dinkgreve[a], Henri de Cagny[a,b], Dion J. Koeze[c], Brian P. Tighe[c], Daniel Bonn[a,*]

[a] Van der Waals-Zeeman Institute, Institute of Physics, University of Amsterdam, Science Park 904, Amsterdam, 1098 XH, The Netherlands
[b] Unilever Research Laboratories, Olivier van Noortlaan 120, 3313 AT Vlaardingen, The Netherlands
[c] Process & Energy Laboratory, Delft University of Technology, Leeghwaterstraat 39, Delft, 2628 CB, The Netherlands

ARTICLE INFO

Keywords:
Yield-stress materials
Rheological measurements
Herschel–Bulkley model
Universal scaling

ABSTRACT

Yield-stress materials form an interesting class of materials that behave like solids at small stresses, but start to flow once a critical stress is exceeded. It has already been reported both in experimental and simulation work that flow curves of different yield-stress materials can be scaled with the distance to jamming or with the confining pressure. However, different scaling exponents are found between experiments and simulations. In this paper we identify sources of this discrepancy. We numerically relate the volume fraction with the confining pressure and discuss the similarities and differences between rotational and oscillatory measurements. Whereas simulations are performed in the elastic response regime close to the jamming transition and with very small amplitudes to calculate the scaling exponents, these conditions are hardly possible to achieve experimentally. Measurements are often performed far away from the critical volume fraction and at large amplitudes. We show that these differences are the underlying reason for the different exponents for rescaling flow curves.

Complex fluids, such as emulsions, suspensions, foams and pastes, form an important class of materials, exhibiting both solid- and liquid-like behaviour. Understanding and predicting the flow behaviour of these complex materials is of industrial and fundamental importance [1,2]. These materials show the emergence of a yield stress for volume fractions above a critical volume fraction ϕ_c, called the jamming transition. At small stresses yield-stress materials behave like solids, deforming in an elastic manner. However, once a critical stress, called the yield stress (σ_y), is exceeded, the material starts to flow. Describing the flow properties of yield-stress materials as a function of the volume fraction has become an important research topic, both in experimental [3–5] and simulation work [6–8]. Universal rescaling of yield stress flow curves would enable us to predict the yield stress of a material when the volume fraction and surface tension are known [4]. Flow curves for concentrated systems with $\phi > \phi_c$ can be described by the Herschel–Bulkley model [9]

$$\sigma = \sigma_y + K\dot{\gamma}^{\beta} \tag{1}$$

where σ is the stress, $\dot{\gamma}$ is the shear rate and K and β are model parameters. The vanishing of the yield stress with decreasing volume fraction can be described as a power law in the distance to jamming

$$\sigma_y = \sigma_0 |\Delta\phi|^{\Delta} \tag{2}$$

with σ_0 a constant on the order of the Laplace pressure of the droplets and $\Delta\phi = \phi - \phi_c$.

There have already been a large number of articles dealing with the scaling of flow curves. Here we give a short overview of the work that has already been done on scaling of flow curves from yield-stress materials. Paredes et al. [4] investigated experimentally the flow properties of one such yield-stress fluid: an emulsion with volume fractions above and below the jamming transition. They were able to scale all flow curves with respect to the volume fraction into two master curves, one for the supercritical and one for the subcritical volume fractions, by plotting $\sigma/|\Delta\phi|^{\Delta}$ versus $\dot{\gamma}/|\Delta\phi|^{\Gamma}$. Similar scaling values were found by Nordstrom et al. [3] and Basu et al. [10] when scaling flow curves of a soft-colloid system.

Paredes et al. [4] interpreted scaling collapse as evidence for a critical transition in the dynamics, from liquid- to solid-like behaviour. In the analogy with equilibrium phase transitions, they supposed that the scaling exponent values are universal, i.e. independent of particle interactions. Subsequent experimental studies provided support for this hypothesis: Dinkgreve et al. [5] found that experimental flow properties of other soft sphere systems, with different interparticle interactions, could also be scaled with power laws in the distance to jamming. The scaling parameters for all different systems have, within numerical uncertainty, the same values of $\Delta \approx 2$ and $\Gamma \approx 4$.

Whereas experimental research on the flow curves of yield-stress materials give similar scaling parameters for soft sphere systems with different interparticle interactions [3–5,10], numerical estimates of the scaling exponents have tended to differ from experiments [7,8,11–16]. For

* Corresponding author.
E-mail addresses: r.i.dekker@uu.nl (R.I. Dekker), d.bonn@uva.nl (D. Bonn).

https://doi.org/10.1016/j.jnnfm.2018.08.006
Received 8 April 2018; Received in revised form 5 July 2018; Accepted 6 August 2018
Available online 14 August 2018
0377-0257/© 2018 Elsevier B.V. All rights reserved.

example, the yield-stress exponent Δ is generally estimated to be lower for particles with harmonic (spring-like) interactions [7,11,12,14], which is believed to be a good model for emulsions [17]. Second, while there is broad agreement that exponents for both static and flow properties are identical in two, three, and four dimensions [6,12,13,15], there is generally a dependence on particle interactions. For example, when elastic quantities such as the confining pressure, shear modulus and yield stress are expressed as power laws in $\Delta\phi$, they scale with different exponents when the particles have harmonic or Hertzian interactions [6,18].

Recently, Dagois-Bohy et al. [8] reported the softening and yielding of soft glassy materials, based on athermal soft sphere simulations of both small and large amplitude oscillatory tests. They showed, amongst other things, scaling of the linear elastic and loss moduli of a two-dimensional system with respect to the quiescent confining pressure P of the system. The results were in good agreement with theoretical models of small amplitude oscillatory shear [16,19]. Data collapse into two master curves, one for the elastic modulus and one for the loss modulus, was found when plotting G^*/P^α versus ω/P^β with $\alpha \approx 0.45$ and $\beta \approx 0.8$, close to the mean field exponents $\alpha = 1/2$ and $\beta = 1$ [8].

When comparing the experimental work of Paredes et al. [4] with the simulation work of Dagois-Bohy et al. [8], some differences are immediately obvious. Whereas similar systems of soft particles with harmonic interactions are studied, different scaling parameters are found. However, the control parameters are also different: in experiments the volume fraction (distance to jamming) that is controlled, whereas in the simulations it is the pressure (distance to jamming) that is the control parameter. The tendency to express numerical scaling relations in terms of the pressure, rather than excess volume fraction is advantageous because (i) the value of the confining pressure at jamming is strictly zero, and therefore known with arbitrary precision, and (ii) the pressure is easily accessible in simulations. A second difference between the simulations and experiments is observed when looking at the type of measurements. While experimental studies of jamming and rheology have focused on continuous flow, simulations mainly used oscillatory shear.

In this paper we ask where the discrepancy between numerical and experimental scaling exponents of flow curves from yield-stress materials comes from. For clarity, we only investigate well-behaved emulsion systems that can be modelled as soft harmonic particles. Therefore we relate the volume fraction of the dispersed phase with the confining pressure, to be able to compare scaling to the volume fraction distance to jamming with the confining pressure. Furthermore, we compare continuous shear experiments with oscillatory experiments. We observe that above yielding, oscillatory and rotational flow curves overlap. Plotting as a function of the confining pressure, the scaling exponents of experimental and numerical work come closer together. However, this does not solve the discrepancy between experimental and numerical scaling exponents. We end this paper with a discussion on the possible explanation that experiments and simulations probe different things and therefore do not have the same scaling exponents.

1. Materials and methods

1.1. Castor oil-in-water emulsions

Mobile castor oil-in-water emulsions stabilized by sodium dodecyl sulphate (SDS) were prepared. For the continuous phase, 1 wt% of SDS (from Sigma-Aldrich) was dissolved in demineralized water. Rhodamine B (from Sigma-Aldrich) was added as a dye. The castor oil (from Sigma-Aldrich) was added to the aqueous phase and stirred with a Silverson L5M-A emulsifier at 8,000 rpm for 6 minutes. The SDS solution was mixed with castor oil in a 1:4 volume ratio to obtain a 80% castor oil-in-water emulsion. This 80% emulsion was diluted with the SDS solution to obtain emulsions with lower ϕ. All samples were centrifuged for 10 minutes at 1000 rpm to remove any air bubbles. The oil droplets have a mean diameter of 3.4 μm with a dispersity of 20%, determined using confocal laser scanning microscopy.

1.2. Rheological measurements

The rheological measurements were performed on an Anton Paar MCR 302 rheometer. A 50 mm-diameter cone-and-plate geometry was used with a 1° cone and roughened surfaces to avoid wall slip [20]. All samples were pre-sheared at a shear rate of 100 s^{-1} for 30 s, followed by a rest period of 30 s to create a controlled initial state in all samples [4]. The rotational tests were performed by carrying out a shear rate sweep from 1000 s^{-1} to $1 \cdot 10^{-3}$ s^{-1}. The oscillatory measurements were performed by carrying out an amplitude sweep from 0.1% to $1 \cdot 10^4$ % at a constant frequency of 1 Hz. A flow curve can be obtained from an oscillatory measurement, using that the shear rate is linear related to the strain amplitude and frequency, $\dot{\gamma} = \gamma\omega$. All measurements were performed at room temperature. The flow curves were fitted to the Herschel–Bulkley model with a weight inversely proportional to the stress, meaning that a larger discrepancy between the fit and the measured value is accepted at higher stress values than at low stress values.

1.3. Numerical data

The relation between the experimental volume fraction of the dispersed phase and the confining pressure is calculated from a standard relation based on the virial, $p = 1/(2V)\sum_{ij} r_{ij} f_{ij}$, where the sum runs over contacting particle pairs, r_{ij} is the centre-to-centre distance between a pair, and f_{ij} is its contact force. The numerical storage and loss moduli as a function of the frequency are generated using an in-house code that uses the non-linear conjugate gradient method to instantaneously quench a periodic system of bidisperse particles from a random configuration to a local minimum of the elastic potential energy landscape. This is the so-called “Ising model of jamming” [21]. Storage and loss moduli are calculated for soft harmonic particles as these best model experimental emulsions and for pressures close to the jamming transition. The numerical frequency was made dimensionless using the droplet size, surface tension and the viscosity.

2. Results

2.1. Volume fraction versus confining pressure

Whereas scaling of experimental flow curves is normally done with a power law in the distance to jamming, $\Delta\phi$, simulation data are scaled with a power law in the confining pressure. Relating the confining pressure with ϕ or $\Delta\phi$ would solve one of the discrepancies that might explain the differences in scaling exponents. A numerical relation between the quiescent (zero shear) confining pressure and the volume fraction for a three-dimensional system with a binary mixture of soft spheres is shown in Fig. 1. Below the critical jamming point, $\phi_c = 0.64$, the confining pressure is zero. While the initial growth of the pressure with $\Delta\phi$ is linear [6], significant corrections to linear scaling are present over the experimentally accessible range of ϕ, as can be seen from the slope of the graph. Therefore, we expect different effective exponents when scaling the flow curves with respect to the confining pressure in comparison with scaling with respect to $\Delta\phi$.

Flow curves for castor oil-in-water emulsions with volume fractions between 68% and 80% are obtained from rotational measurements, see Fig. 2a. The data are fitted to the Herschel–Bulkley model, $\sigma = \sigma_y + K\dot{\gamma}^\beta$ to determine the yield stress. It can directly be seen from the curves in Fig. 2a that the yield stress increases with increasing volume fraction. The volume fractions were converted to confining pressure values using the numerical relation as shown in Fig. 1. The values for the yield stress as obtained from the Herschel–Bulkley fits were plotted against the confining pressure, see Fig. 2b. The blue line shows a linear fit of the data points through the origin. The fit shows a linear relation between the

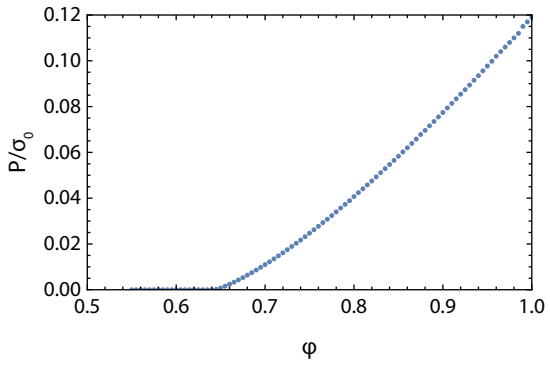

Fig. 1. Numerical relation between the confining pressure and the volume fraction of the dispersed phase for a three-dimensional system. Below the critical volume fraction for jamming, $\phi_c = 0.64$, the pressure is zero.

yield stress and the confining pressure, with the yield stress vanishing at zero confining pressure.

As discussed above, flow curves above the critical jamming volume fraction can collapse into one master branch by plotting $\sigma/\sigma_0|\Delta\phi|^{\Delta}$ versus $\dot{\gamma}/\sigma_0|\Delta\phi|^{\Gamma}$ [4,5]. We divide the stress by the Laplace pressure σ_0 to make the data dimensionless. Consistent with prior work, we find scaling collapse using $\Delta \approx 2.1$ and $\Gamma \approx 3.8$, see Fig. 2c. The errors on Δ and Γ come from small fluctuations in the scaling of the flow curves. Scaling requires $\beta = \Delta/\Gamma \approx 0.55$, and indeed a direct fit to the master curve gives fitting parameters $\beta = 0.56$ and $K = 0.19$.

We now attempt to rescale the flow curves from Fig. 2a with the confining pressure, rather than $\Delta\phi$. The linear relation between the yield stress and the confining pressure, as shown in Fig. 2b, gives the first scaling parameter $a \approx 1$. We find that all data collapses into one master curve by plotting $\sigma/[\sigma_0 P^a]$ versus $\dot{\gamma}/[\sigma_0 P^b]$ with $a = 1.02 \pm 0.02$ and $b = 1.84 \pm 0.22$, see Fig. 2d. The master curve follows the Herschel–Bulkley model with $\beta = a/b = 0.56 \pm 0.07$. This shows that we can scale the flow curves with respect to the distance to jamming, but also with respect to the confining pressure. Note that whereas $a \neq \Delta$ and $b \neq \Gamma$, their ratios a/b and Δ/Γ (which set β) are the same. This is because, precisely at the jamming transition where both P and $\Delta\phi$ are zero, the flow curve is that of a power law fluid $\sigma \propto \dot{\gamma}^{\beta}$. Hence β cannot be sensitive to the choice to rescale with P or $\Delta\phi$.

Scaling the experimental emulsion flow curves with a power law in the confining pressure instead of the volume fraction distance to jamming, brings the scaling parameters closer to the scaling parameters found in simulations. However, for experiments we found scaling exponents $a \approx 1$ and $b \approx 2$, whereas for simulations scaling exponents of $a \approx 1/2$ and $b \approx 1$ are found [8]. Scaling to the confining pressure thus does not solve the discrepancy between experiments and simulations. We therefore have to look further into the control parameters and the differences between experiments and simulations.

2.2. Rotational versus oscillatory measurements

Rotational measurements are the most common way in experimental research to obtain flow curves of emulsions. A shear rate is applied and the stress is measured. However, scaling of simulation data is often ap-

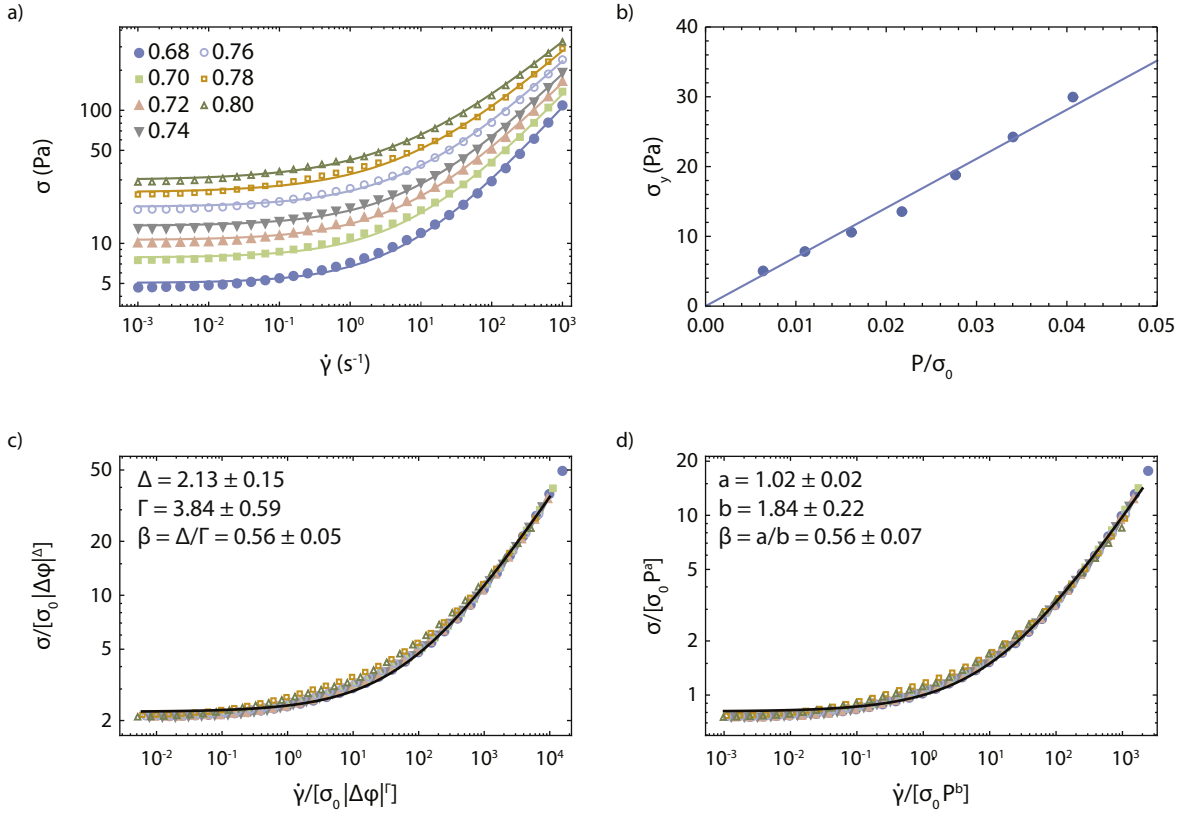

Fig. 2. Rescaling of flow curves of castor oil-in-water emulsions. (a) Flow curves of castor oil-in-water with 1wt% SDS emulsions for volume fractions between 0.68 and 0.80 of the oil phase. The lines show Herschel–Bulkley fittings of the experimental data. (b) Yield stress as a function of pressure with a linear fit through the origin. The yield stress is obtained from Herschel–Bulkley fits of the flow curves as shown in (a). The volume fraction is related to the pressure using the numerical relation as shown in Fig. 1. (c) Master curve showing the collapse of the flow curves into one when plotted as $\sigma/\sigma_0|\Delta\phi|^{\Delta}$ versus $\dot{\gamma}/\sigma_0|\Delta\phi|^{\Gamma}$ with $\Delta = 2.13 \pm 0.15$ and $\Gamma = 3.84 \pm 0.59$. The black line corresponds to a Herschel–Bulkley fit with $\beta = a/b = 0.56$ and $K = 0.19$. (d) Similar to (c) but now plotted as $\sigma/\sigma_0 P^a$ versus $\dot{\gamma}/\sigma_0 P^b$ with $a = 1.02 \pm 0.02$ and $b = 1.84 \pm 0.22$. The black line corresponds to a Herschel–Bulkley fit with $\beta = a/b = 0.56$ and $K = 0.19$.

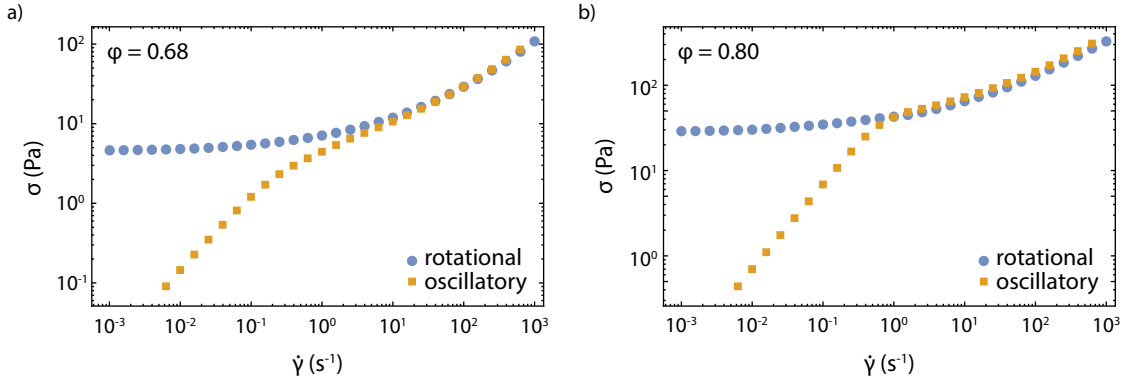

Fig. 3. Shear stress as a function of the shear rate for a castor oil-in-water with 1wt% SDS emulsion with a volume fraction of (a) 0.68 and (b) 0.80 of the oil phase. The circles show a flow curve measured with a rotational test, whereas the squares show a flow curve measured with an oscillatory test. (For interpretation of the references to color in this figure legend, the reader is referred to the web version of this article.)

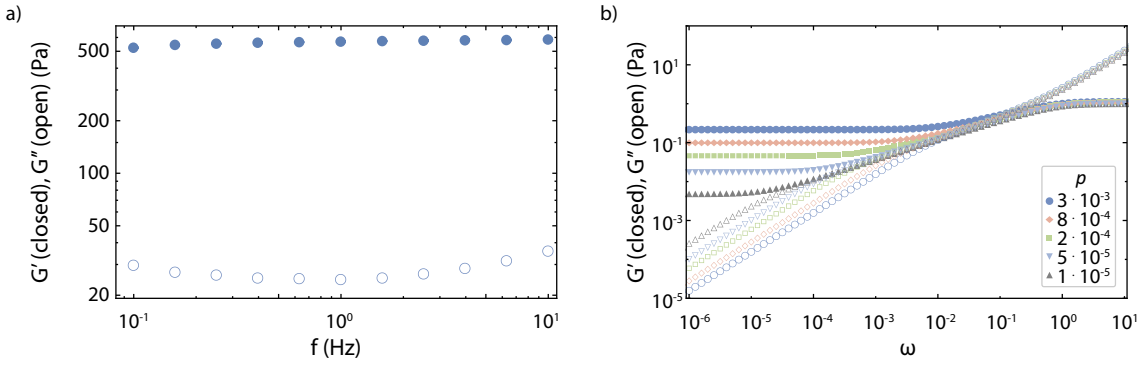

Fig. 4. Comparison between experimental and numerical shear moduli (a) Experimental storage (closed circles) and loss (open circles) moduli as a function of frequency for a 80% castor oil-in-water with 1wt% SDS emulsion. At low frequencies, the storage and loss modulus are independent of frequency. (b) Numerical storage (closed symbols) and loss (open symbols) moduli as a function of dimensionless frequency ω for various confining pressures close to jamming. An increase in the loss modulus is observed with increasing frequency, whereas the storage modulus remains constant in a large range of frequencies.

plied using the storage and loss moduli data [8,19], obtained from oscillatory measurements. These measurements can also be plotted as stress versus shear rate flow curves, which allows us to compare both methods. Flow curves were obtained for castor oil-in-water emulsions with volume fractions of the oil phase between 68% and 80% both from rotational and oscillatory measurements. The results for the emulsions with the lowest (68%) and the highest (80%) volume fractions are shown in Fig. 3. The graphs show a clear overlap between the curves of the rotational and the oscillatory tests at high shear rates ($\dot{\gamma} \gtrsim 1s^{-1}$) above yielding (in the oscillatory tests, we vary $\dot{\gamma}$ by sweeping strain amplitude at fixed frequency). The difference between the flow curves at lower shear rates reflects insufficient strain in the oscillatory measurements to reach a steady flow [22]. The low-shear part of the oscillatory measurements shows the elastic behaviour of the sample.

From the overlap between both flow curves at high shear rates, we can conclude that the same information can be obtained from rotational and oscillatory measurements. Therefore, we do not obtain different scaling exponents if we scale flow curves obtained from oscillatory measurements. The fact that experimental flow curves are measured in continuous shear, whereas numerical flow curves are obtained in oscillatory mode, consequently does not explain the difference between experimental and numerical scaling exponents.

3. Discussion and conclusion

We can conclude that simulations and experiments really show different scaling exponents for the rescaling of flow curves and cannot be assigned to a difference in measurements protocol or control parameters (confining pressure or volume fraction of the dispersed phase). A possible explanation for the discrepancy is then that experiments and simulations probe different things. A direct comparison of oscillatory measurements in experiments and simulations indeed reveals important differences. As can be seen in Fig. 4a, G' and G'' for a 80% castor oil-in-water emulsion are independent of the frequency in the low frequency regime, indicating that they are characterised by a very broad spectrum of visco-elastic relaxation times. Numerical data from soft sphere systems at various confining pressures show no such plateau in G'', see Fig. 4b. Whilst the storage modulus remains constant with increasing frequency, the loss modulus increases and so this system is likely characterised by a narrower distribution of relaxation times. The origin of this discrepancy between experimental and numerical loss moduli is not clear and merits further study.

Another important difference is that in simulations of viscous soft spheres one is able to approach the jamming point much closer than in experiments: they can easily reach excess volume fractions, strain amplitudes, and dimensionless strain rates on the order of 10^{-6} or lower, which is orders of magnitude smaller than typical experimental lower bounds. As a result, simulations and experiments have typically probed different windows of response. This is because the focus of simulations has largely been on determining critical exponents as accurately as possible, which requires approaching ϕ_c as closely as possible.

A difference in material properties of the jammed material, indicated by the frequency-independent loss modulus in experiments and the frequency-dependent loss modulus in simulations, and a difference in the response window could then explain the discrepancy in scaling exponents. However, it is yet unknown how to resolve these differences;

if that could be done, this would be the final step to get similar scaling exponents from both simulations and experiments.

Acknowledgements

This work is part of the research programme Controlling Multiphase Flow with project number 680-91-012, which is (partly) financed by the Netherlands Organisation for Scientific Research (NWO).

References

[1] R.G. Larson, The Structure and Rheology of Complex Fluids, Oxford University Press, 1999.
[2] M.M. Denn, D. Bonn, Issues in the flow of yield-stress liquids, Rheol. Acta 50 (4) (2011) 307–315, doi:10.1007/s00397-010-0504-3.
[3] K.N. Nordstrom, E. Verneuil, P.E. Arratia, A. Basu, Z. Zhang, A.G. Yodh, J.P. Gollub, D.J. Durian, Microfluidic rheology of soft colloids above and below jamming, Phys. Rev. Lett. 105 (17) (2010) 1–4, doi:10.1103/PhysRevLett.105.175701.
[4] J. Paredes, M.A. Michels, D. Bonn, Rheology across the zero-temperature jamming transition, Phys. Rev. Lett. 111 (1) (2013) 1–5, doi:10.1103/PhysRevLett.111.015701.
[5] M. Dinkgreve, J. Paredes, M.A. Michels, D. Bonn, Universal rescaling of flow curves for yield-stress fluids close to jamming, Phys. Rev. E 92 (1) (2015) 012305, doi:10.1103/PhysRevE.92.012305.
[6] C.S. O'Hern, L.E. Silberg, A.J. Liu, S.R. Nagel, Jamming at zero temperature and zero applied stress: the epitome of disorder, Phys. Rev. E 68 (2003) 011306, doi:10.1103/PhysRevE.70.043301.
[7] D. Vågberg, P. Olsson, S. Teitel, Universality of jamming criticality in overdamped shear-driven frictionless disks, Phys. Rev. Lett. 113 (14) (2014) 1–5, doi:10.1103/PhysRevLett.113.148002.
[8] S. Dagois-Bohy, E. Somfai, B.P. Tighe, M. van Hecke, Softening and yielding of soft glassy materials, Soft Matter 13 (47) (2017) 9036–9045, doi:10.1039/C7SM01846K.
[9] W.H. Herschel, R. Bulkley, Konsistenzmessungen von gummi-Benzollösungen, Kolloid Z. 39 (4) (1926) 291–300.
[10] A. Basu, Y. Xu, T. Still, P.E. Arratia, Z. Zhang, K.N. Nordstrom, J.M. Rieser, J.P. Gollub, D.J. Durian, A.G. Yodh, Rheology of soft colloids across the onset of rigidity: scaling behavior, thermal, and non-thermal responses, Soft Matter 10 (17) (2014) 3027–3035, doi:10.1039/c3sm52454j.
[11] P. Olsson, S. Teitel, Critical scaling of shear viscosity at the jamming transition, Phys. Rev. Lett. 99 (17) (2007) 1–4, doi:10.1103/PhysRevLett.99.178001.
[12] M. Otsuki, H. Hayakawa, Critical behaviors of sheared frictionless granular materials near the jamming transition, Phys. Rev. E 80 (1) (2009) 5–10, doi:10.1103/PhysRevE.80.011308.
[13] M. Otsuki, H. Hayakawa, Universal scaling for the jamming transition, Prog. Theor. Phys. 121 (3) (2009) 647–655, doi:10.1143/PTP.121.647.
[14] B.P. Tighe, E. Woldhuis, J.J. Remmers, W. Van Saarloos, M. Van Hecke, Model for the scaling of stresses and fluctuations in flows near jamming, Phys. Rev. Lett. 105 (8) (2010) 1–4, doi:10.1103/PhysRevLett.105.088303.
[15] G. Katgert, B.P. Tighe, M. van Hecke, The jamming perspective on wet foams, Soft Matter 9 (41) (2013) 9739–9746, doi:10.1039/c3sm51543e.
[16] K. Baumgarten, B.P. Tighe, Viscous forces and bulk viscoelasticity near jamming, Soft Matter 13 (45) (2017) 8341–8662, doi:10.1039/C7SM01619K.
[17] D.J. Durian, Foam mechanics at the bubble scale, Phys. Rev. Lett. 75 (26) (1995) 4780–4783, doi:10.1103/PhysRevLett.75.4780.
[18] C. Heussinger, J.L. Barrat, Jamming transition as probed by quasistatic shear flow, Phys. Rev. Lett. 102 (21) (2009) 1–4, doi:10.1103/PhysRevLett.102.218303.
[19] B.P. Tighe, Relaxations and rheology near jamming, Phys. Rev. Lett. 107 (15) (2011) 1–5, doi:10.1103/PhysRevLett.107.158303.
[20] V. Bertola, F. Bertrand, H. Tabuteau, D. Bonn, P. Coussot, Wall slip and yielding in pasty materials, J. Rheol. 47 (5) (2003) 1211–1226, doi:10.1122/1.1595098.
[21] M. Van Hecke, Jamming of soft particles: geometry, mechanics, scaling and isostaticity, J. Phys. Condens. Matter 22 (3) (2010) 1–24, doi:10.1088/0953-8984/22/3/033101.
[22] M. Dinkgreve, M.M. Denn, D. Bonn, "Everything flows?": elastic effects on startup flows of yield-stress fluids, Rheol. Acta 56 (3) (2017) 189–194, doi:10.1007/s00397-017-0998-z.